Published in final edited form as:
Chem Res Toxicol. 2009 September ; 22(9): 1570–1581. doi:10.1021/tx900114v.

Spin Trapping and Cytoprotective Properties of Fluorinated Amphiphilic Carrier Conjugates of Cyclic versus Linear Nitrones

Grégory Durand[*,†], **Robert A. Prosak**[‡], **Yongbin Han**[‡], **Stéphanie Ortial**[†], **Antal Rockenbauer**[¶], **Bernard Pucci**[†], and **Frederick A. Villamena**[*,‡]

[‡] Department of Pharmacology and Center for Biomedical EPR Spectroscopy and Imaging, The Davis Heart and Lung Research Institute, College of Medicine, The Ohio State University, Columbus, OH 43210

[†] Laboratoire de Chimie BioOrganique et des Systèmes Moléculaires Vectoriels, Faculté des Sciences, Université d'Avignon et des Pays de Vaucluse, 33 Rue Louis Pasteur, 84000 Avignon, France

[¶] Chemical Research Center, Institute of Structural Chemistry, H-1025 Budapest, Pusztaszeri 59, Hungary

Abstract

Nitrone spin traps have been employed as pharmacological agent against neurodegenerative diseases and ischemia-reperfusion induced injury. The structure-activity relationship was explored for the two types of nitrones, i.e., cyclic (DMPO) and linear (PBN), which are conjugated to a fluorinated amphiphilic carrier (FAC) for their cytoprotective properties against hydrogen peroxide (H_2O_2), 3-morpholinosynonimine hydrochloride (SIN-1) and 4-hydroxynonenal (HNE) induced cell death on bovine aortic endothelial cells. The compound FAMPO was synthesized and characterized, and its physical-chemical and spin trapping properties were explored. Cytotoxicity and cytoprotective properties of various nitrones either conjugated and non-conjugated to FAC (i.e., AMPO, FAMPO, PBN and FAPBN) were assessed using 3-[4,5-dimethylthiazol-2-yl]-2,5-diphenyltetrazolium (MTT) reduction assay. Results show that of all the nitrones tested, FAPBN is the most protective against H_2O_2, but FAMPO and to a lesser extent its unconjugated form, AMPO, are more protective against SIN-1 induced cytotoxicity. However, none of the nitrones used protect the cells from HNE-induced cell death. The difference in the cytoprotective properties observed between the cyclic and linear nitrones may arise from the differences in their intrinsic antioxidant properties and localization in the cell.

Introduction

Reactive oxygen species (ROS)[1] in low concentrations play an important role in regulating cell function, signaling and immune response (1,2) but in unregulated concentrations are

frederick.villamena@osumc.edu; Tel: +1 614-292-8215; FAX: +1 614-688-0999; gregory.durand@univ-avignon.fr; Tel: +33-4-9014-4445. Fax: +33-4-9014-4441.

Supporting Information Available: ^{1}H NMR and HRMS spectra of AcO-FAMPO; ^{1}H, ^{3}C, DEPT 135, ^{19}F NMR and HRMS spectra of FAMPO; cytotoxicity and cytoprotection data. This material is available free of charge via the Internet at http://pubs.acs.org.

[1]AMPO, 5-carbamoyl-5-methyl-1-pyrroline-*N*-oxide; CMPO, 5-carboxy-5-methyl-1-pyrroline-*N*-oxide; DEPMPO, 5-diethoxyphosphoryl-5-methyl-1-pyrroline-*N*-oxide; DMPO, 5,5-dimethyl-pyrroline *N*-oxide; FAC, N^{α}-Lactobiony-N^{ε}-(benzyloxycarbonyl)-L-lysinyl-1*H*,1*H*,2*H*,2*H*-perfluorooctylamine; FAMPO, N^{α}-Lactobionyl-N^{ε}-(carboxamide-5-methyl-1-pyrroline-*N*-Oxide)-L-lysinyl-1*H*,1*H*,2*H*,2*H*-perfluorooctylamine; FAPBN, N^{α}-lactobionyl-N^{ε}-(*N*-*tert*-butyl-*α*-carboxyphenylnitrone)-L-lysinyl-1*H*,1*H*,2*H*,2*H*-perfluorooctylamine; HNE, 4-hydroxynonenal; MTT, 3-[4,5-dimethylthiazol-2-yl]-2,5-diphenyltetrazolium; PBN, α-phenyl *N*-*tert*-butyl nitrone; SIN-1: 3-morpholinosynonimine hydrochloride, ROS, reactive oxygen species.

detrimental to cell viability due to alteration of the cellular redox state that often leads to oxidative stress. Oxidative stress has been implicated in a large number of pathophysiological disorders such as cardiovascular disease (3), cancer (4), inflammation (5), or ischemia-reperfusion injury (6). The use of natural (7,8) and synthetic (9) antioxidants to attenuate ROS-mediated oxidative stress have been recently gaining significant attention. Of particular interest are nitrone spin traps (Figure 1) which undergo addition reaction with free radicals making them a popular analytical reagent for the identification of short-lived radicals using electron paramagnetic resonance (EPR) spectroscopy (10). The linear nitrone, α-phenyl *N*-*tert*-butyl nitrone (PBN) was also employed as pharmacological agent (11-13) against age-related diseases such as stroke, cancer, Parkinson's and Alzheimer's diseases with disodium-[(*tert*-butylimino)-methyl]benzene-1,3-disulfonate *N*-oxide (NXY-059) being the first neuroprotective agent that has reached phase 3 clinical trial in the USA. Experimental evidences suggest that the pharmacological activity of NXY-059 involves inhibition of signal transduction and gene induction processes leading to apoptosis, and is not solely due to their radical trapping capability. The cyclic nitrone, 5,5-dimethyl-pyrroline *N*-oxide (DMPO) has also been employed as cardioprotective agent against ischemia-reperfusion induced injuries (14). Recently, we demonstrated that introduction of a bolus of DMPO (1 mM) after 30 minutes of ischemia shows cardioprotective properties after 30 minute reperfusion using rat heart Langendorff system (15). This protection is due in part to the salvaging of the mitochondrial electron transport chain system from oxidative damage. However, despite the exceptional ability of nitrones in preventing oxidative stress conditions, the molecular mechanism of their action remains obscure (11,13).

The second order rate constants for the reaction of hydroxyl radical ($HO^{\bullet}$) to PBN and DMPO are in the same range, i.e., 2.7-3.6 × 10^9 $M^{-1}s^{-1}$ and 6.1-8.5 × 10^9 $M^{-1}s^{-1}$, respectively (16), but the rate of $O_2^{\bullet-}$ trapping, however, is orders of magnitude slower with k_2 = 1.7 $M^{-1}s^{-1}$ for DMPO (17) and k_2 = 0.12 $M^{-1}s^{-1}$ for PBN (18). Despite the poor reactivity of PBN and DMPO to $O_2^{\bullet-}$, they have been widely used as protective agents in several biological models of oxidative stress. However, there are other physical-chemical properties of nitrones that could potentially provide new motivation for their application as therapeutic agent. For example, our previous studies showed that cyclic nitrones react with a variety of free radicals at orders of magnitude faster than $O_2^{\bullet-}$ (19), the $O_2^{\bullet-}$ adduct formed decomposes to release NO (20), nitrone reaction with $CO_3^{\bullet-}$ yields nitrite (21) that can increase NO bioavailability upon reaction with heme iron proteins, and that nitrones are more reactive in acidosis conditions, common in ischemic and tumor cells (22).

Amphiphilic compounds possessing both hydrophilic and lipophilic group could exhibit improved cellular permeability, and therefore, several amphiphilic derivatives of PBN such as the fluorinated amphiphilic PBN conjugate FAPBN (Figure 1), have been developed as potential therapeutic agents (23,24) or modification of these amphiphiles with technetium-chelating sites has found application as non-proteic probes for hepatocyte PET imaging (25). However, amphiphilic compounds with a long hydrogenated tail (i.e., 8 carbons or more) are detergent by nature and lead to disruption of cell membranes when used above their critical micellar concentration (cmc). This limitation is overcome with the use of fluorinated tails. Indeed, perfluorinated amphiphiles have very little cytolytic effect compared to hydrogenated amphiphiles due to the non miscibility of the fluorinated chain with the hydrogenated chain of phospholipids (26). Because of their lyophobic properties, surfactants with fluorinated chains do not partition well into biological membrane and therefore are expected to cross cell membrane easily without inducing toxicity.

As additional potential benefits brought by fluorinated compounds, one can expect a prolonged *in vivo* half-life (27), enhanced bioavailability (23,28) as well as detection via ^{19}F NMR for pharmacokinetic monitoring (29). Indeed, highly fluorinated amphiphilic amino acids have

been shown to increase the protective activity of different antioxidants and particularly that of nitrones (23) without demonstrating any cytotoxicity. Increasing nitrone bioavailability through improved cellular permeability may offer a more robust pharmacological activity in *in vitro* and *in vivo* models (30-35). Selective targeting is usually achieved by conjugating the nitrones to target-specific ligands. In addition to the type of ligands that are tethered to nitrones, it has been demonstrated that the nature of the linker group also affects its bioactivity (23). Therefore, the nature of the linker group, the target specificity as well as the efficiency of radical trapping have to be considered in the design of new spin traps with improved antioxidant properties.

While cyclic nitrones such as DMPO (36) and 5-diethoxyphosphoryl-5-methyl-1-pyrroline-*N*-oxide (DEPMPO) (37) have been widely employed as spin trapping agents with more superior properties than that of PBN-type nitrones in terms of reactivity to $O_2^{\bullet -}$ and $HO_2^{\bullet}$, there is no reported study on cyclic nitrones conjugated to amphiphilic groups. Moreover, the nature of $HO_2^{\bullet}$ addition to PBN and its derivatives was found to be electrophilic, while the addition of $O_2^{\bullet -}$ to PBN-type compounds is only weakly electrophilic (18), in contrast to the $O_2^{\bullet -}$ addition to DMPO-type compounds which is nucleophilic in nature (17). It is therefore important to investigate the relative cytoprotective properties of these two major types of nitrones against some oxidants. Herein, we report the synthesis of a new fluorinated amphiphilic cyclic nitrone, FAMPO (Figure 1). The self-aggregation behavior of FAMPO in water, its spin trapping properties as well as its cytoprotective property against various oxidants were investigated and compared to that of FAPBN.

Experimental Procedures

Synthesis

The precursors AcO-FAC (23) and CMPO (38) were prepared according to published procedures. All reagents were used as purchased without further purification. All solvents were distilled and dried according to standard procedures. TLC analyses were performed on silica gel 60F254 pre-coated sheets and detection was carried out using UV light (254 nm), ninhydrin solution (for amine-containing compound detection) or *p*-anisaldehyde stain (for glycolipid detection) with heating at 150 °C. Flash column and size exclusion chromatography were carried out using silica gel (200-400 mesh) and Sephadex LH 20 resin, respectively. Infrared spectra were recorded as pressed solids using an attenuated total reflectance IR spectrometer. ^{1}H, ^{19}F and ^{13}C NMR spectra were recorded using either 400 or 250 MHz spectrometer.

N$^{\alpha}$-(2,3,4,6,2′,3′,4′,6′-O-Acetyllactobionyl)-*N*$^{\varepsilon}$-(carboxamide-5-methyl-1-pyrroline-*N*-Oxide)-L-lysinyl-1*H*,1*H*,2*H*,2*H*-perfluorooctylamine (AcO-FAMPO)

To a solution of AcO-FAC (180 mg, 0.138 mmol) in ethanol/acetic acid (99:1 v/v), 15 mg of 10% Pd/C was slowly added at 0 °C. The mixture was transferred to a Parr apparatus and catalytic hydrogenation was performed for 12 h at 7 bar pressure. The crude mixture was filtered through Celite pad and the solvent was evaporated *in vacuo*. Under N_2 atmosphere, the resulting amino compound dissolved in a minimum amount of dry CH_2Cl_2 was added, to a solution of CMPO (27 mg, 0.187 mmol), EDC (35 mg, 0.187 mmol), HOBt (5 mg, 0.035 mmol) also in dry CH_2Cl_2 containing 2 drops of TEA (pH ~ 8-9). The reaction mixture was stirred and the progress of reaction was monitored by TLC (EtOAc/MeOH/H_2O 7:2:1 v/v/v for monitoring AcO-FAC consumption and MeOH/CH_2Cl_2 10:1 v/v for monitoring compound formation) until all of the AcO-FAC was consumed. Solvent was immediately removed *in vacuo* and the crude mixture was purified by flash column chromatography using CH_2Cl_2/MeOH (94:6 v/v) as eluent to give AcO-FAMPO (120 mg, 0.093 mmol, 67% yield) as a white solid. ^{1}H NMR (400 MHz, CDCl3) δ 1.24 (t, J = 6.8 Hz, 2H), 1.35 (m, 2H), 1.57-1.65 (m, 4H),

1.71 (d, *J* = 7.2 Hz, 2H), 1.89 (m, 2H), 2.00-2.30 (m, 20 H), 2.30-2.47 (m, 3H), 2.68 (m, 2H), 3.05 (m, 1H), 3.20-3.40 (m, 2H), 3.58 (m, 2H), 3.77 (m, 1H), 3.92 (m, 1H), 4.10 (m, 2H), 4.22 (m, 3H), 4.60 (m, 2H), 5.03 (m, 1H), 5.17 (m, 2H), 5.36 (m, 2H), 5.62 (m, 1H), 6.76 (m, 1H), 6.86 (m, 1H), 7.08 (m, 1H), 8.37-8.49 (m, 1H). HRMS calcd for $C_{48}H_{61}F_{13}N_4O_{22}Na$ ($M+Na^+$) *m/z* 1315.3468, found 1315.3406.

N^{α}-Lactobionyl-N^{ε}-(carboxamide-5-methyl-1-pyrroline-*N*-Oxide)-L-lysinyl-1*H*,1*H*,2*H*,2*H*-perfluorooctylamine (FAMPO)

To a solution of AcO-FAMPO (120 mg, 0.093 mmol) in dry MeOH, a catalytic amount of NaOMe was added under N_2 atmosphere. The mixture was stirred for 4 h and 1 N HCl solution was added drop-wise to neutralize the solution and then the solvents were evaporated *in vacuo*. The resulting crude mixture was purified by size exclusion chromatography using MeOH as eluent. Precipitation in Et_2O afforded FAMPO (64 mg, 0.067 mmol, 72 % yield) as a white solid. ^{1}H NMR (250 MHz, CD_3OD) δ 1.30-1.85 (m, 8H), 1.85-2.02 (m, 1H), 2.18-2.32 (m, 1H), 2.32-2.60 (m, 2H, C$\underline{H}_2$-CF_2), 2.76 (m, 2H), 3.28 (t, *J* = 6.7 Hz, 2H), 3.45-4.05 (m, 12H), 4.23 (dd, *J* = 2.1, 4.3 Hz, 1H), 4.38 (dd, *J* = 4.65, 9.4 Hz, 1H), 4.45 (m, 1H), 4.52 (d, *J* = 7.3 Hz, 1H), 7.51 (bs, C$\underline{H}$=N(O), 1H). ^{13}C NMR (62.86 MHz, CD3OD) δ 21.0, 22.7, 25.8, 28.3, 29.5, 29.8, 30.9, 31.3, 31.4, 38.9, 52.9, 61.3, 62.4, 68.9, 71.4, 71.8, 72.8, 73.4, 75.9, 79.4, 81.8, 104.4, 145.7, 170.4, 172.8, 174.2. ^{19}F NMR (235 MHz, CD_3OD) δ -82.3 (3 F, C$\underline{F}_3$), -115.3 (2 F, C$\underline{F}_2$-CH_2), -122.9 (2 F, C$\underline{F}_2$), -123.9 (2 F, C$\underline{F}_2$), -124.6 (2 F, C$\underline{F}_2$), -127.3 (2 F, C$\underline{F}_2$-CF_3). IR (Neat, cm^{-1}) ν 3318, 1652, 1539, 1436, 1233, 1199, 1144, 1122, 1075, 1018. HRMS calcd for $C_{32}H_{45}F_{13}N_4O_{14}Na$ ($M+Na^+$) *m/z* 979.2622, found 979.2602.

Computational Studies

All calculations were performed at the Ohio Supercomputer Center. The minimization of initial structures using MMFF94 (39) were performed with MacroModel 9.6 (40). Conformational search was then carried out using MMFF94 via Monte Carlo Multiple Minimum method coupled with Generalized Born/Surface Area (GB/SA) continuum solvation model using water as the solvent (41) as implemented in the MacroModel package. The preferred geometries obtained from the first conformational search were further subjected to conformational search at least twice by employing the exact procedure mentioned above. Geometry optimization was further carried out using Hartree-Fock (HF) self-consistent field method at the HF/6-31G* level of theory using Gaussian 03 (42). Bottom-of-the-well energies were obtained using single point calculation at the HF/6-31G* level and polarizable continuum model (PCM) (43-47) using the solvation effects of water or heptane. The Cartesian coordinates were generated using the GaussView 3.0 Program.

Determination of log k'_W Values

Methanol solutions of the compounds (1.0 mg/mL) were injected to an HPLC equipped with Microsorb C18 column (250 mm × 4.6 mm, 5μm). The compounds were eluted at various MeOH and water ratios (9:1 to 3:7 v/v) using a flow rate of 0.8 mL/min. The column temperature was 25 °C, and the UV detector wavelengths used were λ = 298 nm for PBN and FAPBN and 231 nm for DMPO and FAMPO. Linear regression analysis were performed on five data points for PBN (from 8:2 to 4:6; r^2 = 0.9932); four points for DMPO (from 6:4 to 3:7; r^2 = 0.9708); three points for FAPBN (from 9:1 to 7:3; r^2 = 0.9979) and FAMPO (from 8:2 to 6:4, r^2 = 0.9998). The log *k*' values were calculated by using the equation: log *k*' = log $((t-t_0)/t_0)$, where *t* is the retention time of the nitrone and t_0 is the elution time of MeOH, which is not retained in the column.

Particle Size Analyses

The hydrodynamic particle size distributions and polydispersity of amphiphilic nitrones at different concentrations were determined by using a Zetasizer Nano-S model 1600 (Malvern Instruments Ltd., U.K.) equipped with a He-Ne laser (λ= 633 nm, 4.0 mW). In a typical experiment, stock solutions (10 mM) in milli-Q water (resistivity 18.2 mΩ.cm) were prepared and stored at room temperature overnight before measurements. The solutions were then passed through a 0.45 μm filter, a low-volume quartz batch volume was filled with 100 μL of the stock solution, and the size of the particles was measured 1h after filtration, and then solutions were gradually diluted. The time-dependent correlation function of the scattered light intensity was measured at a scattering angle of 173° relative to the laser source. The hydrodynamic radius (R) of the particles was estimated from their diffusion coefficient (D) using the Stokes-Einstein equation, $D = k_B T/6\pi\eta R$, where k_B is the Boltzmann's constant, T is the absolute temperature, and η is the viscosity of the solvent.

EPR Measurements

EPR measurements were carried out on a Bruker EMX-X band with an HS resonator at room temperature. General instrument settings were as follows: microwave power, 10 mW; microwave frequency, 9.87 GHz; modulation amplitude, 1.0 G; sweep width, 100-120 G; time constant, 20.48 ms; sweep time, 40.96 s; receiver gain, 10^3-10^5. Sample cells used were 50 μL quartz or glass capillary tubes for UV or non-UV irradiation experiments, respectively. The spectral simulations were carried out using an automatic fitting program (48).

Spin Trapping

(a) Hydroxyl Radical. Using low-pressure mercury vapor lamp at 254 nm, hydroxyl radical was generated by irradiation of a mixture of nitrone (20 mM) and H_2O_2 (0.5%) solution in PBS solution (pH 7.0). In the second experiment, 60% dioxane was added before irradiation. **(b) Superoxide radical anion.** (*i*) *KO_2 generating system*. To a 40 μL solution of the nitrone in DMSO was added 10 μL of the supernatant from a saturated solution of KO_2 in DMSO to give a final nitrone concentration of 10 mM FAMPO or 115 mM FAPBN. (*ii*) *Pyridine/H_2O_2 system*. Pyridine solution of nitrone (10 mM) containing 230 mM H_2O_2 was used. **(c) Methoxy radical.** Methoxy radical was generated by adding ~1 mg of solid $Pb(OAc)_4$ to a DMSO solution of nitrone (20 mM) containing 10% v/v of MeOH. **(d) *tert*-Butoxy radical.** *tert*-Butoxy radical was generated by UV irradiation of the nitrone (10 mM FAMPO and 20 mM FAPBN) and 80 mM (*tert*-BuO)$_2$ solution in DMSO. **(e) Pentyl radical.** Pentyl radical was generated by UV irradiation of 20 mM nitrone and 80 mM pentyl iodide solution in DMSO.

Determination of Nitrone Concentrations after Incubation with Cells

Cells were incubated with 50 μM of nitrone at 0, 4, 6 or 24 h, and the media (50 or 100 μL using linear or cyclic nitrones, respectively) was injected to an HPLC equipped with Apollo C18 column (150 mm × 4.6 mm, 5μm). The compounds were eluted at various MeOH and water ratios (80:20 to 20:80) using a flow rate of 0.75 mL/min (1.0 mL/min was used for DMPO). The column temperature was 25 °C, and the UV detector wavelengths used were λ = 295 nm for PBN and FAPBN, and 235 nm for DMPO and FAMPO. For controls, HPLC analyses were carried out on the media in the presence of cells alone. No degradation was also observed for all the nitrones upon 24 h incubation in the media alone. All concentrations were based on the peak area of a 50 μM concentration of the respective nitrone standard.

Cytoprotective Studies

(a) Cell culture—All reagents or materials were purchased and used without further purification. Bovine aortic endothelial cells (BAEC) were purchased from Cell Systems (Kirkland, WA). Cells were cultured in 75 cm^2 tissue culture flasks using Dulbecco's modified

eagle medium with 4.5 g/L D-glucose, 4 mM L-glutamine and supplemented with 10% fetal bovine serum, 2.5 mg/L endothelial cell growth supplement, and 1% non-essential amino acids (Gibco) in the absence of antibiotics at 37°C in a humidified atmosphere of 5% CO_2 and 20% O_2. The medium was changed every 2-3 days and cells were sub-cultured once they reached 90–95% confluence.

(b) 3-[4,5-Dimethylthiazol-2-yl]-2,5-diphenyltetrazolium (MTT) reduction assay —Cytotoxicity of SIN-1, H_2O_2 and HNE, and the cytoprotective properties of the nitrones against these pro-oxidative agents were assessed using MTT assay. In a typical experiment, using 24-well culture plates, BAEC cells were incubated at 37°C in the presence of 0.01 to 1.0 mM concentrations of the nitrone for 24 h in DMEM media supplemented with 0.5% FBS and 25 mM HEPES. After incubation, known concentrations of SIN-1, H_2O_2 or HNE were added to the well plates and incubated for an additional 24 h (or 6 h in the case of SIN-1). A 0.5 mL solution of MTT (0.45 mg/mL in DMEM supplemented with 0.5% FBS) was then added to each well. Cells were incubated for another 2 h at 37 °C. After the 2 h incubation, the media were removed and wells were rinsed once with DPBS. A 0.3 mL mixture of dimethyl sulfoxide, isopropanol and deionized water (1:4:5 v/v/v) was added to each well at room temperature to solubilize the formazan crystals. The dissolved formazan was then transferred into semi-micro cuvettes, and the absorbance was measured at 570 nm using a spectrophotometer.

Stock alkaline solution (0.3 M NaOH) of sodium peroxynitrite (NaONOO) was prepared. For the cell studies, the final NaOH concentration was ~5 mM and the toxicity of this NaOH solution alone was also assessed and found to convey no significant toxicity. The concentration of the stock solutions of NaONOO was determined by first diluting 25 μl of the stock solution into 975 μl of 0.3 M NaOH and measuring the absorbance at 302 nm immediately after thawing before each experiment. The concentration was then calculated by using the extinction coefficient for $ONOO^-$ ($\varepsilon = 1670\ M^{-1}cm^{-1}$).

(c) Statistical Analysis—Statistical analysis was performed using the student t-test. Statistical significance was considered at $P < 0.05$.

Results and Discussion

Synthesis

The synthesis for FAPBN is discussed elsewhere (23). The synthetic scheme for FAMPO from fluorinated amphiphilic carrier (AcO-FAC) (23) and CMPO (38) is shown in Scheme 1. Briefly, the synthesis of AcO-FAC is based on three key steps from commercially available 1*H*,1*H*,2*H*,2*H*-perfluorooctyliodide. First, the iodo group was converted into an amino group by substitution with a large excess of sodium azide followed by catalytic hydrogenation. Condensation of the resulting 1*H*,1*H*,2*H*,2*H*-perfluorooctylamine to N^{α}-tert-butyloxycarbonyl-N^{ε}-benzyloxycarbonyl-L-lysine is achieved in the presence of DCC/HOBt as coupling reagents. Finally, Boc deprotection was carried out in acidic condition, followed by condensation reaction with lactobionic acid, and acetylation of the hydroxyl groups gave AcO-FAC. Deprotection of the lysine group was achieved by catalytic hydrogenation and the resulting amino compound was reacted with CMPO. The coupling reaction of CMPO with AcO-FAC was demonstrated to be efficient using EDC/HOBt and led to ~67% yield for AcO-FAMPO but poorer yield was obtained using DCC (less than 20% yield). The resulting product, AcO-FAMPO, was found to decompose on longer reaction time and it is necessary to isolate AcO-FAMPO using column chromatography as soon as the reaction has completed within approximately 3~3.5 h. Deacetylation of AcO-FAMPO by the Zemplén procedure and further purification using size exclusion chromatography gave the final product. Characterization by ^1H, ^{13}C, ^{19}F and DEPT-135 NMR as well as by IR and HRMS spectroscopy (see Supporting

Information) were carried out and results were consistent with the FAMPO structure. Procedure similar to that for the deprotection of AcO-FAMPO was employed for the synthesis of FAC.

Molecular Modeling

MFF94 conformational search using the GB/SA continuum solvation model was performed for FAMPO and FAPBN structures and further optimization at the HF/3-21g* level of theory gave conformations as shown in Figure 2. Results show that the conformation of FAPBN is more folded compared to FAMPO where the hydrophilic groups (i.e., nitrone and sugar moieties) in FAMPO are well separated from the lipohilic perfluoroalkyl chain. The calculated relative bottom-of-the-well energies in heptane versus in water showed preference in water for both FAMPO and FAPBN but a significantly higher energy difference was observed in heptane for FAMPO (15.9 kcal/mol) versus FAPBN (5.0 kcal/mol) indicating that FAMPO is significantly more polar than FAPBN.

Physical-chemical Measurements

Since the biological effects of nitrone analogs are influenced by their lipophilicity (31,49) as previously demonstrated, we therefore measured the relative lipophilicity of the two fluorinated amphiphilic nitrones by chromatographic technique. DMPO and PBN were also included for the sake of comparison and results are shown in Table 1. Similar to that reported using other techniques (Table 1), the lipophilicity of the PBN was found to be much higher than that of DMPO with log k'_W value of 1.64 and 0.31, respectively. As expected, the amphiphilic fluorinated nitrones were found to be more lipophilic than their unconjugated form, while FAPBN is more lipophilic than FAMPO with log k'_W values of 5.10 and 4.03, respectively. It has to be emphasized that in spite of the high lipophilicity of both FAPBN and FAMPO, they were found to be readily soluble in water up to 50 mM. The higher lipophilicty of FAPBN and FAMPO compared to their parent compounds may provide improved permeability to membranes and thus enhance cytoprotection.

Using dynamic light scattering (DLS) method, the self-aggregation of FAMPO in water was studied and compared with FAPBN. As shown in Table 2 and Figure S8, both amphiphilic nitrones formed aggregates of ~5 nm diameter which could be spherical micelles as we previously observed for fluorinated surfactants (50) and in full agreement with this assumption, FAPBN was shown to form micelles at a concentration of 0.05 mM (23) demonstrating that the observed aggregates are micellar by nature. Although the two amphiphilic nitrones share the same fluorinated glycolipidic amphiphilic carrier, the self-aggregation properties of these two compounds are slightly different. First, while stable aggregates of FAPBN were observed in the range of 0.5-10 mM, no stable micellar aggregates were observed for FAMPO below 2.5 mM. The stronger self-aggregation behaviour of the PBN derivative is in agreement with its higher lipophilicity as demonstrated by the partition coefficient values (Table 1). Keeping in mind the cmc value of FAPBN, it shows that high concentrated solutions of surfactant are needed to observe stable micellar aggregates. Second, the hydrodynamic diameter of FAMPO aggregates is lightly smaller than that of FAPBN with 7-23% differences. According to the Israelachvili's concept (51,52) where the volumetric ratio between the polar head and the hydrophobic tail of a surfactant influences the nature and size of its aggregates formed in aqueous solutions suggests that the volume of the polar head of FAMPO could be larger than that of FAPBN. As recently reported for glucose-based fluorinated surfactants (50), such a decrease in the aggregate diameter as the volume of the polar head increases suggest that in aqueous solution, the DMPO moiety may be oriented towards the side of the lactobionamide polar head than the lipophilic fluorinated group, a hypothesis consistent with the optimized HF/3-21g* conformations of FAMPO as shown in Figure 2. However, for FAPBN, the molecule assumes a more folded conformation.

To further study the conformation of FAMPO in solution, 2D-NMR nuclear Overhauser enhancement spectroscopy (NOESY) was used to investigate the through-space dipolar interaction between the protons of the nitrone moiety and that of the sugar moiety within 5 Å (53). However, no long range correlation peaks can be found either in MeOD or in D_2O (Data not shown). This may suggest that the DMPO nitrone moiety is not close enough (within 5 Å) to the galactose-based hydrophilic head regardless of the solvent used indicating a weak interaction between these two moieties in solution.

EPR Spin Trapping Studies

To evaluate the spin trapping ability of FAMPO and FAPBN, we investigated the formation of its adduct with various radicals using EPR as shown in Figures 3-5 while Table 3 shows the EPR parameters from simulation. Chiral nitrones give two diastereoisomeric adducts, i.e., *cis*- and *trans*- isomers (17). Since the nitrones are racemic, four diastereoisomeric radical adducts can be formed (i.e., *R-cis*, *S-cis*, *R-trans* and *S-trans* products) but we only carried out the EPR spectral simulation using one species for simplicity, unless otherwise indicated.

(a) Hydroxyl Radical—Hydroxyl radical adduct was generated from UV photolysis of the spin trap in the presence of H_2O_2. However, only weak signals were observed for FAMPO and FAPBN as shown in Figure 3. The FAMPO-OH spectrum shows considerable linewidth broadening and asymmetry characteristic of a slow molecular tumbling motion. However, higher anisotropy was observed for FAPBN-OH due perhaps to a more extensive self-aggregation of FAPBN-OH compared to FAMPO-OH in aqueous phase which follows the aggregation behaviors of FAPBN and FAMPO. The restricted rotational motion of amphiphilic fluorinated nitrone spin adducts has already been observed and was explained as a result of the micellar aggregate formation (54). The addition of 60% of dioxane to the buffer solution gave isotropic spectra for both nitrones demonstrating the non-favorability of supramolecular organization in the presence of dioxane, and therefore, allows for the free molecular tumbling of the nitroxide as previously demonstrated (54).

(b) Superoxide Radical Anion—Generation of $O_2^{\bullet-}$ adduct in aqueous phase using xanthine/xanthine oxidase only gave weak EPR signal (data not shown) but the $O_2^{\bullet-}$ adduct formation in non-aqueous solvents gave stronger EPR signals regardless of $O_2^{\bullet-}$ generating system used (Figure 4). However, it is interesting to note that 10 mM of the nitrones gave a strong signal using pyridine/H_2O_2 but considerably weaker EPR signal was obtained using DMSO/KO_2 at the same nitrone concentration, or at even higher concentration (~ 115 mM) in the case of FAPBN. The difference in the yields of adduct formation from using pyridine/H_2O_2 compared to DMSO/KO_2 could be due to the difference in polarity and reactivity of the radical generated from these two systems, that is, $HO_2^{\bullet}$ and $O_2^{\bullet-}$, respectively (18). Since $HO_2^{\bullet}$ is a stronger oxidizer than $O_2^{\bullet-}$ ($E^{o\prime}$ = 1.06 and 0.94 V, respectively (55)), and while the rate constants of $HO_2^{\bullet}$ addition to nitrones is higher compared to $O_2^{\bullet-}$ (17,56,57), it is expected that the relative yields of the adducts originating from $HO_2^{\bullet}$ or $O_2^{\bullet}$ can be thermodynamically and kinetically affected.

(c) Miscellaneous Radicals—Methoxy, pentyl and *tert*-butoxy radical adducts of both FAMPO and FAPBN were also generated. As shown in Figure 5 and Table 3, FAMPO gave more discernable spectra for various adducts compared to FAPBN. However, molecular tumbling is more affected in FAPBN adducts at higher field compared to FAMPO adducts indicating differences in their polarities hence the aggregation properties of these two sets of adduct.

Stability and Internalization of Nitrone Compounds

The stability of 50 μM AMPO, DMPO, PBN, FAMPO and FAPBN in culture media for 24 h at 37 °C was assayed by HPLC. No degradation was observed during this incubation time demonstrating that all the compounds are chemically stable under these conditions. HPLC analysis of the supernatant after incubation with BAEC was followed over a 24 h period (Figure 6 and Figure S9). Because of the overlapping peaks between AMPO and with those from the media, the concentrations for AMPO were not determined. After only 4 h of incubation, a dramatic decrease in the concentrations of PBN and FAPBN was observed while lower but significant in the concentration of DMPO was observed after 24 h. Suprisingly, the concentration of FAMPO only dropped by 20% after 4 h and then remained constant over the 24 h of incubation. This decrease in the extracellular nitrone concentrations in the presence of BAEC could be due mostly to the internalization of the compounds into the cells. This suggests that the PBN-derivatives might be able to favorably compartmentalize into the cells and that the internalization is slightly favored by the carrier. However, the data from FAMPO indicates that this compound does not compartmentalize very well into the cell even after 24 h of incubation and in spite of the very close lipophilicity values of FAMPO and FAPBN, this observation is quite unexpected. It seems that the cylic nitrone moiety exhibits a lower propensity to cross cell membrane than linear nitrones and affects the ability of the carrier to compartmentalize due perhaps to the competing properties of these two groups or the overall conformation of FAMPO in solution that does not allow facile diffusion into the cell. Since the transport mechanism through the cell membrane may involve more than one mode, that is, via passive diffusion, endocytosis, membrane fusion, pores and/or receptor-proteins, differences in compartmentalization behavior may arise in spite of similar lipophilicity of FAMPO and FAPBN.

Cytoprotective Properties

Cytotoxicity of nitrone compounds and oxidants—The cytotoxicity of all nitrones including that of the FAC alone on BAEC was investigated in the 0.025-1 mM concentration range and results are reported in Table 4. Using concentrations up to 1 mM, the nitrones AMPO, DMPO, PBN and FAPBN were found to exhibit no cytotoxicity while FAMPO showed a 20% and 53% decrease in cell viability at 0.5 and 1mM, respectively. The de-*O*-acetylated carrier, FAC, gave cell toxicity of ~5-28% at a concentration range of 0.025-1.0 mM. However, a similar carrier with a two-carbon longer fluorinated chain and an acetamido group in place of the benzyl carbamate protective group was found to be non-toxic at 500 mg/kg after i.v. administration to mice (28). This suggests that the Z-protective group may be the origin of the toxicity. This may also explain why the toxicity of the carrier is sharply diminished when nitrone compounds are grafted through the amide bond. The cytotoxicity of various oxidants were also investigated, and H_2O_2 was found to decrease cell viability by 95% at a concentration of 180 μM (Figure S10) while SIN-1 was found to decrease cell viability by 93% at a concentration of 600 μM. (Figure S11). The lipid peroxidation product, 4-hydroxynonenal (HNE), was found to decrease cell viability by 95% at 50 μM (Figure S12).

Cytoprotection against H_2O_2 toxicity—Hydrogen peroxide has been suggested to cross mammalian cell membranes (58) and to the inner mitochondrial membrane (59) via specific aquaporins. The H_2O_2 induced toxicity is due to a myriad of different mechanisms that include various pathways such as those associated with translocation of the mitochondrial pro-apoptotic BAX proteins, upregulation of p53, loss of mitochondrial membrane potential, cytochrome-*c* release, caspase-3 activation, PARP cleavage, and DNA fragmentation (60). Moreover, H_2O_2 can activate protein kinases that can lead to apoptosis (60). All the nitrones at 25 μM showed cytoprotection against 180 μM of H_2O_2 and no statistical significance in cell viability was observed between the nitrone-H_2O_2 treated cells and that of the untreated cells (Figure 7). Furthermore, as shown in Figures 6 and 7, both cyclic and linear nitrones offered

extracellular and intracellular protection against H_2O_2 induced toxicity, respectively. The potency of the nitrone compounds is demonstrated here as they antagonize the H_2O_2 induced cell death at a 7-fold lower concentration than that of the oxidant. This is in agreement with previous findings by Joseph et al. (61), showing that PBN protects against H_2O_2-induced cytotoxicity using PC12 cells. Cell viability results from FAC treatment alone were not statistically significant compared to H_2O_2 treatment alone which demonstrates the ineffectiveness of the carrier itself to impart cytoprotection against H_2O_2-induced toxicity (Figure 7). However, at 10 μM concentrations of the nitrones, only FAPBN showed robust protection against H_2O_2 ($P < 0.05$, versus control untreated) compared to other nitrones. The protection afforded by FAPBN at low concentration is in agreement with the previous data on primary cortical mixed cultures demonstrating its high potency in preventing the H_2O_2 induced toxicity (23). The robustness of FAPBN protection compared to that of PBN may be due to its ability to preferentially compartmentalize intracellularly.

The effect of short incubation time against the H_2O_2-induced cell death was also investigated with FAPBN to simulate acute conditions during oxidative injury. Cells were incubated with FAPBN for 15 min before being exposed to H_2O_2 for 24 h and results are presented in Figure S13. Protection was significantly lower by ~ 50% than that observed after 24 h of incubation. Some rationale for nitrone protection against H_2O_2 were demonstrated by Floyd et al. (62) in stroke models showing that PBN can inhibit gene induction of heat shock proteins, *c-fos* and inducible nitric oxide synthase as well as signal transduction processes in neurodegenerative events. For example, p38 pathway activation has been shown to be inhibited by PBN due to suppression of IL-1β or H_2O_2 and with concomitant increase in phosphatase activity suggesting the role of ROS as second messenger molecule in signal transduction processes (62). Moreover, previous studies have shown that PBN may undergo decomposition to form *tert*-butyl hydroxylamine and can be further oxidized to *tert*-butylnitroso compound leading to NO formation in biological models under oxidative stress conditions (63). The enhanced antioxidant properties of PBN-type compounds against H_2O_2 toxicity may therefore arise either from their metabolites or via suppression of signal transduction and gene induction processes leading to apoptosis as shown by Floyd, et al. Furthermore these mechanisms may explain the limited protection observed after a short incubation time.

Cytoprotection against SIN-1 toxicity—Figure 8 shows the cytoprotective properties of various nitrones against SIN-1 induced toxicity. Results show that the cyclic nitrones, FAMPO (25 and 100 μM) and AMPO (100 μM) offers protection against SIN-1 compared to the linear nitrones, FAPBN, PBN, and FAC alone. Because of the low toxicity of PBN and FAPBN, their cytoprotective properties were investigated at 0.5 and 1 mM, and no protection was observed even at these high concentrations (Figure S14). The mechanism of SIN-1 induced cell death has not been fully elucidated although SIN-1 has been suggested to induce cell death via two mechanisms, that is, production of peroxynitrite ($ONOO^-$) through reaction between $NO^\bullet$ and $O_2^{\bullet -}$ to finally form $HO^\bullet$ (64,65) and production of H_2O_2 caused by the reaction of a decomposition product of SIN-1 with HEPES (66). Since our compounds were tested in the presence of a high HEPES concentration (25 mM), this could also result in the formation of H_2O_2 (66) along with $ONOO^-$. Peroxynitrite has been implicated in a variety of pathophysiological conditions perhaps through protein nitration, thiol oxidation, enzyme cofactor oxidation, or NFκB activation, resulting in impaired phase 2 enzymes activity, glutathione depletion, eNOS uncoupling, or enhanced inflammatory responses, respectively, to name a few. On the other hand, $ONOO^-$ was found to be able to induce damages to the mitochondrial electron transport chain (ETC) as it can diffuse through cell membranes or anion channels to cause mitochondria damage (67). The protection exhibited by FAMPO and AMPO against SIN-1 induced toxicity may be due to their ability to act extracellularly from SIN-1 decomposition products before the reactive species enter the cells. However, since H_2O_2 and $ONOO^-$ can also diffuse through cell membranes, the inability of PBN-derivatives to protect

regardless of the concentration used suggests that the intrinsic antioxidant properties of linear nitrones are different from that of the cyclic ones.

The effect of short incubation time of FAPBN against SIN-1 was also investigated. Cells were incubated with FAPBN at concentration range of 25-500 μM for 15 min before being exposed to 600 μM SIN-1 for 6 h but results show no cell protection, confirming the inefficacy of FAPBN to protect BAEC from SIN-1 regardless of the concentration or the incubation time. Also, as shown in Figure S16, addition of relatively low amount of catalase significantly decrease the toxicity of SIN-1 as no cell death was detected up to 600 μM of SIN-1 whereas at the same concentration of SIN-1 without catalase (Figure S11), the cell viability was found to be less than 10%. This proves that H_2O_2 production is involved in the toxicity of SIN-1 in agreement with the literature further confirming the co-operative action between NO and H_2O_2 in SIN-1 toxicity (68). The involvement of H_2O_2 production was also demonstrated by Trakey et al. who observed that the addition of SOD to neuronal cells augmented SIN-1-mediated toxicity (69). To confirm if the observed trend in cytroprotection by the linear and cyclic nitrones against SIN-1 will follow that of using NaONOO, a direct $ONOO^-$ source, using HEPES-free media, cells were incubated in the absence or presence of nitrones for 15 min before exposing to a toxic concentration of $ONOO^-$ (i.e., ~500 μM) (Figure S18) for another 6 h. Due to the limited quantity of FAMPO during this experiment, only PBN, FAPBN and AMPO were tested and compared for their cytotoxicity. Figure S19 shows that the same trend in cytoprotection can be observed in which the cyclic nitrone, AMPO, exhibits dose dependence protection while no protection was observed from using increasing concentrations of PBN and FABN. These results indicate that the toxicity observed from SIN-1 mostly originates from $ONOO^-$ and that H_2O_2 plays a minor role in the SIN-1 induced toxicity.

Finally, to verify the extracellular nature (Figure 6) of the cyclic nitrones protection against SIN-1, 100 μM of FAMPO and AMPO were incubated for 24 h with cells and then the extracellular media was removed, the cells were then washed once before adding SIN-1. This procedure allowed us to remove the nitrones that remained in the extracellular matrix after 24 h of incubation. The cell viability was determined 24 h after the addition of SIN-1 and the results are shown in Figure S17. For both compounds, no statistically significant protection was observed compared to untreated cells, which is in stark contrast with high protection observed without washing. This latter result suggests that AMPO and FAMPO, due to their extracellular distribution as demonstrated by HPLC, protect the cells from extracellular damages mediated by SIN-1 and may act directly as spin traps against $O_2^{\bullet -}$ or $ONOO^-$toxicity. A rationale as to why cyclic nitrones can trap SIN-1 derived radicals whose concentrations can be several fold higher than the cyclic nitrone concentration is probably due to the higher reactivity of the radicals with the spin adducts. Samuni and co-workers (70-72) showed the antioxidant properties of nitroxides either as SOD-mimetics or direct radical scavengers. Since spin adducts are nitroxides by nature, we expect that these adducts are also capable of further reacting with the highly oxidizing species, $HO^{\bullet}$ and NO_2, which are the main by-products of $ONOO^-$ decomposition. This extracellular protection offered by cyclic nitrones is relevant for the prevention of oxidative stress from exogenously generated radicals since for example, leukocytes and phagocytes, via NADPH oxidase activation may affect adjacent cells. Furthermore, extracellular generation of ROS is important in the development of atherosclerosis and may have implications in NO bioavailability in the vasculature during ischemia-reperfusion injuries.

Cytoprotection against HNE toxicity—HNE has been shown to react with various nucleophiles, such as thiols from peptides and proteins, as well as guanine in nucleotides, forming Michael adducts (73) which can cause oxidative stress. Moreover, HNE treatment of cells can induce ROS production through post-translational protein modification (74). Cytoprotection of nitrones against HNE was therefore investigated and results show that none

of the nitrones tested showed protection at concentrations up to 1 mM against 50 μM of HNE (Figure 9). Millimolar concentrations of HNE have been shown to be acutely toxic to mammalian cells and can lead to cell death within 1 h. Significant differences in toxicity levels exist however between cell types but most have found the toxicity to be in the 10 to 100 μM range (75-78). A rationale for the poor nitrone protection against HNE-induced cell death could be due to the poor localization of these spin traps to the site of HNE-mediated injury, poor reactivity of the spin traps to reactive species generated from HNE, or non-reactivity of aldehyde with nitrones. This observation is supported by others showing that classical radical scavengers such as Vitamin E do not protect cells from HNE-mediated cell injuries (79). The fact that nitrones (or their metabolites) were not able to prevent cell death from exogenously introduced HNE but were able to protect cells from either SIN-1 or H_2O_2, suggests that nitrones or their metabolites protect cells directly from ROS or can prevent other ROS-induced pro-apoptotic events as shown by others (11).

Conclusion

A novel amphiphilic nitrone antioxidant, FAMPO, possessing a lactobionic polar head, a perfluorinated hydrophobic tail and a lysine scaffold moiety conjugated to a cyclic nitrone was synthesized and characterized. The physical-chemical and spin trapping properties of FAMPO as well as cytoprotective activities were investigated and compared to that of its PBN analogue, FAPBN. FAMPO and FAPBN are both soluble in water but are more lipophilic compared to their parent compounds, DMPO and PBN, respectively. Moreover, these amphiphilic nitrones self-organize in millimolar concentration range in water due to their lipophilicity, with FAPBN we observed a more pronounced self-organization behavior than FAMPO which correlates well with the lipophilicity of their respective nitrone group. Molecular modeling studies show that the bottom-of-the-well energies suggest that FAPBN is more preferred in heptane compared to FAMPO. Although both FAMPO and FAPBN gave spin adducts with oxygen- and carbon-centered radicals as observed using EPR, the FAMPO spin adducts gave more discernable spectra compared to those of the FAPBN spin adducts. Moreover, higher anisotropy was observed for the spin adducts of FAPBN than for FAMPO consistent with the aggregation properties already observed of FAMPO and FAPBN alone in water. FAPBN gave the most robust protection against H_2O_2-induced toxicity to BAEC while FAMPO was found to be protective against $ONOO^-$ but none of the nitrone compounds were protective against HNE. These results suggest that cyclic- and linear-type may exhibit different antioxidant properties. In addition, HPLC analyses of the extracellular matrix suggest that the localization of the amphiphilic nitrones, FAMPO and FAPBN, can be influenced by the nature of the nitrone moiety itself, with FAMPO mainly localizing extracellularly while FAPBN rapidly compartmentalizing into the cells. Such differences in their localization properties may also explain the difference in their mode of cytoprotection against oxidants. While the linear nitrones or their metabolites exhibit intracellular antioxidant properties against H_2O_2, the cyclic nitrones may extracellularly act directly as spin traps against the $ONOO^-$ toxicity. The rational for the significantly different cytoprotective properties of cyclic versus linear nitrones and their cellular target specificity against H_2O_2 and $ONOO^-$ provide new leads in the design of nitrone-based antioxidants with more robust pharmacological properties and warrants further investigation.

Supplementary Material

Refer to Web version on PubMed Central for supplementary material.

Acknowledgments

This work is supported by NIH grant HL081248 and by “Association Française contre les Myopathies” grant 12674. The Ohio Supercomputer Center (OSC) is acknowledged for generous computational support of this research. Stéphanie Ortial acknowledges grants from “Région Provence Alpes Côte d'Azur” and TS Pharma. We thank Fanny Choteau for her technical assistance in the determination of some of the partition coefficient values.

References

1. Nishikawa T, Edelstein D, Du XL, Yamagishi SI, Matsumura T, Kaneda Y, Yorek MA, Beebe D, Oates PJ, Hammes HP, Giardino I, Brownlee M. Normalizing mitochondrial superoxide production blocks three pathways of hyperglycemic damage. Nature 2000;404:787–791. [PubMed: 10783895]
2. Nemoto S, Takeda K, Yu ZX, Ferrans VJ, Finkel T. Role for mitochondrial oxidants as regulators of cellular metabolism. Mol Cell Biol 2000;20:7311–7318. [PubMed: 10982848]
3. Gutierrez J, Ballinger SW, Darley-Usmar VM, Landar A. Free radicals, mitochondria, and oxidized lipids. The emerging role in signal transduction in vascular cells. Circ Res 2006;99:924–932. [PubMed: 17068300]
4. Dreher D, Junod AF. Role of oxygen free radicals in cancer development. Eur J Cancer 1996;32A:30–38. [PubMed: 8695238]
5. Petrone WF, English DK, Wong K, McCord JM. Free radicals and inflammation: superoxide-dependent activation of a neutrophil chemotactic factor in plasma. Proc Natl Acad Sci USA 1980;77:1159–1163. [PubMed: 6928666]
6. Zweier JL, Talukder MAH. The role of oxidants and free radicals in reperfusion injury. Cardiovasc Res 2006;70:181–190. [PubMed: 16580655]
7. Kaliora AC, Dedoussis GVZ, Schmidt H. Dietary antioxidants in preventing atherogenesis. Atherosclerosis 2006;187:1–17. [PubMed: 16313912]
8. Carr A, Frei B. The role of natural antioxidants in preserving the biological activity of endothelium-derived nitric oxide. Free Radical Biol Med 2000;28:1806–1814. [PubMed: 10946222]
9. Moosmann B, Behl C. Antioxidants as Treatment for Neurodegenerative Disorders. Expert Opin Investig Drugs 2002;11:1407–1435.
10. Villamena FA, Zweier JL. Detection of Reactive Oxygen and Nitrogen Species by EPR Spin Trapping. Antioxid Redox Signaling 2004;6:619–629.
11. Floyd RA, Kopke RD, Choi CH, Foster SB, Doblas S, Towner RA. Nitrones as therapeutics. Free Radical Biol Med 2008;45:1361–1374. [PubMed: 18793715]
12. Maples KR, Green AR, Floyd RA. Nitrone-related therapeutics: potential of NXY-059 for the treatment of acute ischaemic stroke. CNS Drugs 2004;18:1071–1084. [PubMed: 15581379]
13. Floyd RA, Hensley K, Forster MJ, Kelleher-Andersson JA, Wood PL. Nitrones, their value as therapeutics and probes to understand aging. Mech Ageing Dev 2002;123:1021–1031. [PubMed: 12044951]
14. Tosaki A, Blasig IE, Pali T, Ebert B. Heart protection and radical trapping by DMPO during reperfusion in isolated working rat hearts. Free Radical Biol Med 1990;8:363–372. [PubMed: 2165975]
15. Zuo L, Chen YR, Reyes LA, Lee HL, Chen CL, Villamena FA, Zweier JL. The Radical Trap 5,5-Dimethyl-1-pyrroline N-oxide Exerts Dose-Dependent Protection Against Myocardial Ischemia-Reperfusion Injury Through Preservation of Mitochondrial Electron Transport. J Pharmacol Exp Ther. 200910.1124/jpet.108.143479
16. Rosen, GMB.; Bradley, E.; Halpern, Howard J.; Pou, Sovitj. Free Radicals: Biology and Detection By Spin Trapping. Oxford University Press; New York: 1999.
17. Villamena FA, Xia S, Merle JK, Lauricella R, Tuccio B, Hadad CM, Zweier JL. Reactivity of Superoxide Radical Anion with Cyclic Nitrones: Role of Intramolecular H-Bond and Electrostatic Effects. J Am Chem Soc 2007;129:8177–8191. [PubMed: 17564447]
18. Durand G, Choteau F, Pucci B, Villamena FA. Reactivity of superoxide radical anion and hydroperoxyl radical with alpha-phenyl-N-tert-butylnitrone (PBN) derivatives. J Phys Chem A 2008;112:12498–12509. [PubMed: 18998656]

19. Villamena FA, Hadad CM, Zweier JL. Comparative DFT Study of the Spin Trapping of Methyl, Mercapto, Hydroperoxy, Superoxide, and Nitric Oxide Radicals by Various Substituted Cyclic Nitrones. J Phys Chem A 2005;109:1662–1674. [PubMed: 16833491]
20. Locigno EJ, Zweier JL, Villamena FA. Nitric oxide release from the unimolecular decomposition of the superoxide radical anion adduct of cyclic nitrones in aqueous medium. Org Biomol Chem 2005;3:3220–3227. [PubMed: 16106305]
21. Villamena FA, Locigno EJ, Rockenbauer A, Hadad CM, Zweier JL. Theoretical and Experimental Studies of the Spin Trapping of Inorganic Radicals by 5,5-Dimethyl-1-Pyrroline N-Oxide (DMPO). 2 Carbonate Radical Anion J Phys Chem A 2007;111:384–391.
22. Burgett RA, Bao X, Villamena FA. Superoxide Radical Anion Adduct of 5,5-Dimethyl-1-pyrroline N-Oxide (DMPO). 3 Effect of Mildly Acidic pH on the Thermodynamics and Kinetics of Adduct Formation. J Phys Chem A 2008;112:2447–2455. [PubMed: 18303874]
23. Ortial S, Durand G, Poeggeler B, Polidori A, Pappolla MA, Boeker J, Hardeland R, Pucci B. Fluorinated Amphiphilic Amino Acid Derivatives as Antioxidant Carriers: A New Class of Protective Agents. J Med Chem 2006;49:2812–2820. [PubMed: 16640342]
24. Ouari O, Polidori A, Pucci B, Tordo P, Chalier F. Synthesis of a Glycolipidic Amphiphilic Nitrone as a New Spin Trap. J Org Chem 1999;64:3554–3556. [PubMed: 11674480]
25. Richard C, Chaumet-Riffaud P, Belland A, Parat A, Contino-Pepin C, Bessodes M, Scherman D, Pucci B, Mignet N. Amphiphilic perfluoroalkyled carbohydrates as new tools for liver imaging. Int J Pharm. 2009in press
26. Chabaud E, Barthélémy P, Mora N, Popot JL, Pucci B. Stabilization of integral membrane proteins in aqueous solutions using fluorinated surfactants. Biochimie 1998;80:515–530. [PubMed: 9782390]
27. Hsieh KH, Needleman P, Marshall GR. Long-acting angiotensin II inhibitors containing hexafluorovaline in position 8. J Med Chem 1987;30:1097–1100. [PubMed: 3585907]
28. Périno S, Contino-Pépin C, Jasseron S, Rapp M, Maurizis JC, Pucci B. Design, synthesis and preliminary biological evaluations of novel amphiphilic drug carriers. Bioorg Med Chem Lett 2006;16:1111–1114. [PubMed: 16386903]
29. Wolf W, Presant CA, Waluch V. 19F-MRS studies of fluorinated drugs in humans. Adv Drug Deliv Rev 2000;41:55–74. [PubMed: 10699305]
30. Asanuma T, Yasui H, Inanami O, Waki K, Takahashi M, Iizuka D, Uemura T, Durand G, Polidori A, Kon Y, Pucci B, Kuwabara M. A New Amphiphilic Derivative, *N*-{[4-(Lactobionamido)methyl] benzylidene}- 1,1-dimethyl-2-(octylsulfanyl)ethylamine *N*-Oxide, Has a Protective Effect Against Copper-Induced Fulminant Hepatitis in Long-Evans Cinnamon Rats at an Extremely Low Concentration Compared with Its Original Form alpha-Phenyl-*N*-(*tert*-butyl) Nitrone. Chemistry & Biodiversity 2007;4:2253–2267. [PubMed: 17886845]
31. Durand G, Poeggeler B, Boeker J, Raynal S, Polidori A, Pappolla MA, Hardeland R, Pucci B. Fine-Tuning the Amphiphilicity: A Crucial Parameter in the Design of Potent alpha -Phenyl-N-tert-butylnitrone Analogues. J Med Chem 2007;50:3976–3979. [PubMed: 17649989]
32. Durand G, Polidori A, Ouari O, Tordo P, Geromel V, Rustin P, Pucci B. Synthesis and preliminary biological evaluations of ionic and nonionic amphiphilic alpha-phenyl-N-tert-butylnitrone derivatives. J Med Chem 2003;46:5230–5237. [PubMed: 14613325]
33. Durand G, Polidori A, Salles JP, Pucci B. Synthesis of a new family of glycolipidic nitrones as potential antioxidant drugs for neurodegenerative disorders. Bioorg Med Chem Lett 2003;13:859–862. [PubMed: 12617908]
34. Poeggeler B, Durand G, Polidori A, Pappolla MA, Vega-Naredo I, Coto-Montes A, Böker J, Hardeland R, Pucci B. Mitochondrial medicine: neuroprotection and life extension by the new amphiphilic nitrone LPBNAH acting as a highly potent antioxidant agent. J Neurochem 2005;95:962. [PubMed: 16135084]
35. Tanguy S, Durand G, Reboul C, Polidori A, Pucci B, Dauzat M, Obert P. Protection Against Reactive Oxygen Species Injuries in Rat Isolated Perfused Hearts: Effect of LPBNAH, a New Amphiphilic Spin-Trap Derived from PBN. Cardiovascular Drugs and Therapy 2006;20:147. [PubMed: 16534547]
36. Finkelstein E, Rosen GM, Rauckman EJ. Spin trapping. Kinetics of the reaction of superoxide and hydroxyl radicals with nitrones. J Am Chem Soc 1980;102:4994–4999.

37. Frejaville C, Karoui H, Tuccio B, le Moigne F, Culcasi M, Pietri S, Lauricella R, Tordo P. 5-Diethoxyphosphoryl-5-methyl-1-pyrroline N-oxide (DEPMPO): a new phosphorylated nitrone for the efficient in vitro and in vivo spin trapping of oxygen-centered radicals. J Chem Soc Chem Commun 1994:1793–1794.
38. Tsai P, Elas M, Parasca AD, Barth ED, Mailer C, Halpern HJ, Rosen GM. 5-Carboxy-5-methyl-1-pyrroline N-oxide: a spin trap for the hydroxyl radical. J Chem Soc Perkin Trans 2001;2:875–880.
39. Halgren TA. Merck Molecular Force Field. I. Basis, Form, Scope, Parameterization and Performance of MMFF94. J Comput Chem 1996;17:490–519.
40. MacroModel 9.6. Schrödinger, LLC; New York, NY: 2005.
41. Still WC, Tempczyk A, Hawley RC, Hendrickson T. Semianalytical treatment of solvation for molecular mechanics and dynamics. J Am Chem Soc 1990;112:6127–6129.
42. Frisch, MJ.; Trucks, GW.; Schlegel, HB.; Scuseria, GE.; Robb, MA.; Cheeseman, JR.; Montgomery, JA., Jr; Vreven, T.; Kudin, KN.; Burant, JC.; Millam, JM.; Iyengar, SS.; Tomasi, J.; Barone, V.; Mennucci, B.; Cossi, M.; Scalmani, G.; Rega, N.; Petersson, GA.; Nakatsuji, H.; Hada, M.; Ehara, M.; Toyota, K.; Fukuda, R.; Hasegawa, J.; Ishida, M.; Nakajima, T.; Honda, Y.; Kitao, O.; Nakai, H.; Klene, M.; Li, X.; Knox, JE.; Hratchian, HP.; Cross, JB.; Bakken, V.; Adamo, C.; Jaramillo, J.; Gomperts, R.; Stratmann, RE.; Yazyev, O.; Austin, AJ.; Cammi, R.; Pomelli, C.; Ochterski, JW.; Ayala, PY.; Morokuma, K.; Voth, GA.; Salvador, P.; Dannenberg, JJ.; Zakrzewski, VG.; Dapprich, S.; Daniels, AD.; Strain, MC.; Farkas, O.; Malick, DK.; Rabuck, AD.; Raghavachari, K.; Foresman, JB.; Ortiz, JV.; Cui, Q.; Baboul, AG.; Clifford, S.; Cioslowski, J.; Stefanov, BB.; Liu, G.; Liashenko, A.; Piskorz, P.; Komaromi, I.; Martin, RL.; Fox, DJ.; Keith, T.; Al-Laham, MA.; Peng, CY.; Nanayakkara, A.; Challacombe, M.; Gill, PMW.; Johnson, B.; Chen, W.; Wong, MW.; Gonzalez, C.; Pople, JA. Gaussian 03. Gaussian, Inc; Pittsburgh PA: 2003.
43. Barone V, Cossi M, Tomasi J. A new definition of cavities for the computation of solvation free energies by the polarizable continuum model. J Chem Phys 1997;107:3210–3221.
44. Barone V, Cossi M, Tomasi J. Geometry optimization of molecular structures in solution by the polarizable continuum model. J Comput Chem 1998;19:404–417.
45. Cossi M, Barone V, Cammi R, Tomasi J. Ab initio study of solvated molecules: a new implementation of the polarizable continuum model. Chem Phys Lett 1996;255:327–335.
46. Tomasi J, Mennucci B, Cammi R. Quantum Mechanical Continuum Solvation Models. Chem Rev 2005;105:2999–3093. [PubMed: 16092826]
47. Tomasi J, Persico M. Molecular Interactions in Solution: An Overview of Methods Based on Continuous Distributions of the Solvent. Chem Rev 1994;94:2027–2094.
48. Rockenbauer A, Korecz L. Automatic computer simulations of ESR spectra. Appl Magn Reson 1996;10:29–43.
49. Ohlweiler DF, Taylor VL, Schmidt CJ. Radical Trapping and Inhibition of Iron-Dependent CNS Damage by Cyclic Nitrone Spin Traps. J Neurochem 1997;68:1173–1182. [PubMed: 9048764]
50. Abla M, Durand G, Pucci B. Glucose-Based Surfactants with Hydrogenated, Fluorinated, or Hemifluorinated Tails: Synthesis and Comparative Physical-Chemical Characterization. J Org Chem 2008;73:8142–8153. [PubMed: 18823145]
51. Israelachvili, JN. Intermolecular and Surface Forces. Vol. 2nd. Academic Press; San Diego: 1992.
52. Nagarajan R. Molecular Packing Parameter and Surfactant Self-Assembly:The Neglected Role of the Surfactant Tail. Langmuir 2002;18:31–38.
53. Schneider HJ, Hacket F, Ruediger V, Ikeda H. NMR Studies of Cyclodextrins and Cyclodextrin Complexes. Chem Rev 1998;98:1755–1785. [PubMed: 11848948]
54. Chalier F, Ouari O, Tordo P. ESR study of spin-trapping with two glycosylated analogues of PBN able to target cell membrane lectins. Org Biomol Chem 2004;2:927–934. [PubMed: 15007424]
55. Buettner GR. The pecking order of free radicals and antioxidants: Lipid peroxidation, α-tocopherol and ascorbate. Arch Biochem Biophys 1993;300:535–543. [PubMed: 8434935]
56. Allouch A, Lauricella RP, Tuccio BN. Effect of pH on superoxide/hydroperoxyl radical trapping by nitrones: an EPR/kinetic study. Mol Phys 2007;105:2017–2024.
57. Villamena FA, Merle JK, Hadad CM, Zweier JL. Rate Constants of Hydroperoxyl Radical Addition to Cyclic Nitrones: A DFT Study. J Phys Chem A 2007;111:9995–10001. [PubMed: 17845014]

58. Bienert GP, Moller AL, Kristiansen KA, Schulz A, Moller IM, Schjoerring JK, Jahn TP. Specific aquaporins facilitate the diffusion of hydrogen peroxide across membranes. J Biol Chem 2007;282:1183–1192. [PubMed: 17105724]
59. Calamita G, Ferri D, Gena P, Liquori GE, Cavalier A, Thomas D, Svelto M. The inner mitochondrial membrane has aquaporin-8 water channels and is highly permeable to water. J Biol Chem 2005;280:17149–17153. [PubMed: 15749715]
60. Ryter SW, Kim HP, Hoetzel A, Park JW, Nakahira K, Wang X, Choi AMK. Mechanisms of Cell Death in Oxidative Stress. Antioxid Redox Signaling 2007;9:49–89.
61. Joseph JA, Strain JG, Jimenez ND, Fisher D. Oxidant injury in PC12 cells-a possible model of calcium "dysregulation" in aging: I. Selectivity of protection against oxidative stress. J Neurochem 1997;69:1252–1258. [PubMed: 9282950]
62. Floyd RA, Hensley K. Reactive Oxygen Species: Nitrone inhibition of age-associated oxidative damage. Ann New York Acad Sci 2000;899:222–237. [PubMed: 10863542]
63. Chamulitrat W, Parker CE, Tomer KB, Mason RP. Phenyl N-Tert-Butyl Nitrone Forms Nitric Oxide as a Result of Its Fe(Iii)-Catalyzed Hydrolysis Or Hydroxyl Radical Adduct Formation. Free Radical Research 1995;23:1–14. [PubMed: 7647915]
64. Beckman JS, Beckman TW, Chen J, Marshall PA, Freeman BA. Apparent hydroxyl radical production by peroxynitrite: implications for endothelial injury from nitric oxide and superoxide. Proc Natl Acad Sci USA 1990;87:1620–1624. [PubMed: 2154753]
65. Ishii M, Shimizu S, Momose K, Yamamoto T. SIN-1-induced cytotoxicity in cultured endothelial cells involves reactive oxygen species and nitric oxide: protective effect of sepiapterin. J Cardiovasc Pharmacol 1999;33:295–300. [PubMed: 10028940]
66. Lomonosova EE, Kirsch M, Rauen U, De Groot H. The critical role of Hepes in SIN-1 cytotoxicity, peroxynitrite versus hydrogen peroxide. Free Radical Biol Med 1998;24:522–528. [PubMed: 9559863]
67. Szabo C, Ischiropoulos H, Radi R. Peroxynitrite: biochemistry, pathophysiology and development of therapeutics. Nature Rev Drug Discovery 2007;6:662–680.
68. Ioannidis, l; de Groot, H. Cytotoxicity of nitric oxide in Fu5 rat hepatoma cells: evidence for co-operative action with hydrogen peroxide. Biochem J 1993;296:341–345. [PubMed: 8257422]
69. Trackey JL, Uliasz TF, Hewett SJ. SIN-1-induced cytotoxicity in mixed cortical cell culture: peroxynitrite-dependent and -independent induction of excitotoxic cell death. J Neurochem 2001;79:445–455. [PubMed: 11677273]
70. Goldstein S, Samuni A, Merenyi G. Reactions of nitric oxide, peroxynitrite, and carbonate radicals with nitroxides and their corresponding oxoammonium cations. Chem Res Toxicol 2004;17:250–257. [PubMed: 14967013]
71. Goldstein S, Samuni A, Russo A. Reaction of cyclic nitroxides with nitrogen dioxide: the intermediacy of the oxoammonium cations. J Am Chem Soc 2003;125:8364–8370. [PubMed: 12837108]
72. Samuni A, Goldstein S, Russo A, Mitchell JB, Krishna MC, Neta P. Kinetics and mechanism of hydroxyl radical and OH-adduct radical reactions with nitroxides and with their hydroxylamines. J Am Chem Soc 2002;124:8719–8724. [PubMed: 12121116]
73. Uchida K. 4-Hydroxy-2-nonenal: a product and mediator of oxidative stress. Prog Lipid Res 2003;42:318–343. [PubMed: 12689622]
74. Whitsett J, Picklo MJ Sr, Vasquez-Vivar J. 4-Hydroxy-2-nonenal increases superoxide anion radical in endothelial cells via stimulated GTP cyclohydrolase proteasomal degradation. Arterioscler Thromb Vasc Biol 2007;27:2340–2347. [PubMed: 17872449]
75. Fukuda A, Osawa T, Hitomi K, Uchida K. 4-Hydroxy-2-nonenal cytotoxicity in renal proximal tubular cells: protein modification and redox alteration. Arch Biochem Biophys 1996;333:419–426. [PubMed: 8809082]
76. Ishimura A, Ishige K, Taira T, Shimba S, Ono SI, Ariga H, Tezuka M, Ito Y. Comparative study of hydrogen peroxide- and 4-hydroxy-2-nonenal-induced cell death in HT22 cells. Neurochem Int 2008;52:776–785. [PubMed: 17977619]
77. Kokubo J, Nagatani N, Hiroki K, Kuroiwa K, Watanabe N, Arai T. Mechanism of destruction of microtubule structures by 4-hydroxy-2-nonenal. Cell Struct Funct 2008;33:51–59. [PubMed: 18360009]

78. Li Y, Cao Z, Zhu H, Trush MA. Differential roles of 3H-1,2-dithiole-3-thione-induced glutathione, glutathione S-transferase and aldose reductase in protecting against 4-hydroxy-2-nonenal toxicity in cultured cardiomyocytes. Arch Biochem Biophys 2005;439:80–90. [PubMed: 15946642]

79. Subramaniam R, Koppal T, Green M, Yatin S, Jordan B, Drake J, Butterfield DA. The free radical antioxidant vitamin E protects cortical synaptosomal membranes from amyloid beta-peptide(25-35) toxicity but not from hydroxynonenal toxicity: relevance to the free radical hypothesis of Alzheimer's disease. Neurochem Res 1998;23:1403–1410. [PubMed: 9814551]

80. Bardelang D, Charles L, Finet JP, Jicsinszky L, Karoui H, Marque SRA, Monnier V, Rockenbauer A, Rosas R, Tordo P. a-phenyl-N-tert-butylnitrone-type derivatives bound to b-cyclodextrins: syntheses, thermokinetics of self-inclusion and application to superoxide spin-trapping. Chem Eur J 2007;13:9344–9354.

81. Janzen EG, West MS, Kotake Y, DuBose CM. Biological spin trapping methodology. III. Octanol-water partition coefficients of spin-trapping compounds. J Biochem Biophys Meth 1996;32:183–190. [PubMed: 8844325]

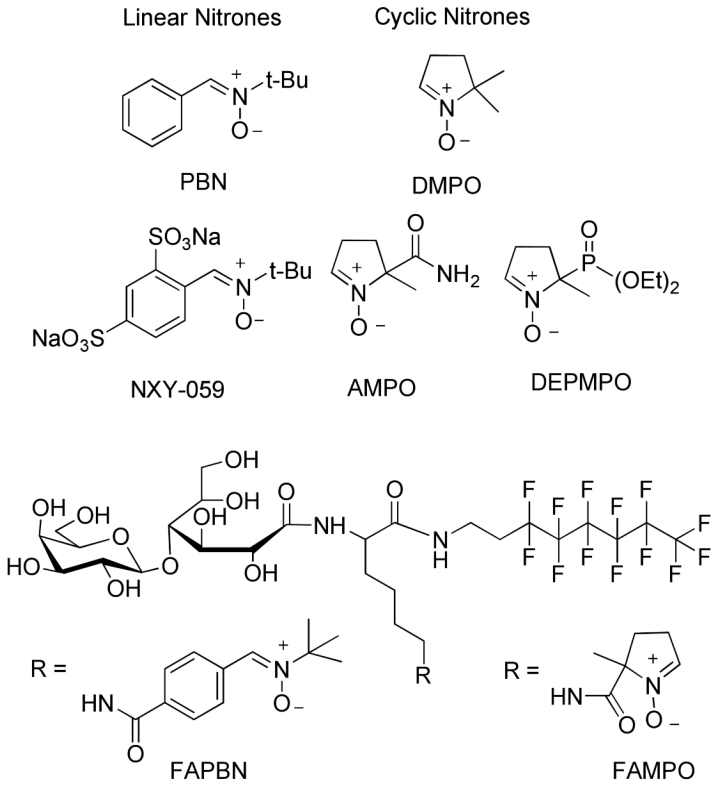

Figure 1.
Examples of cyclic and linear nitrones, and structures of FAPBN and FAMPO.

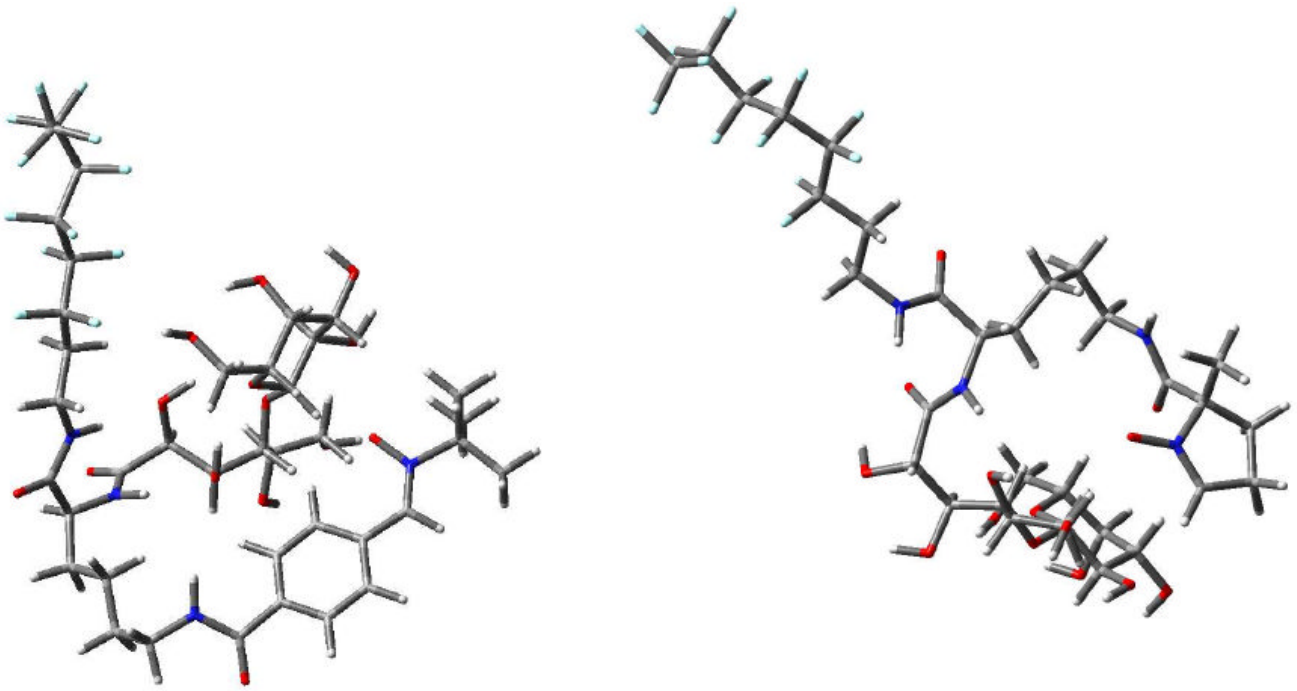

FAPBN

$\Delta E_{rel,heptane} = 5.0$
$\Delta E_{rel,water} = 0.0$

FAMPO

$\Delta E_{rel,heptane} = 15.9$
$\Delta E_{rel,water} = 0.0$

Figure 2.
Lowest energy conformations of FAPBN (left) and FAMPO (right) at the HF/3-21g* level of theory. Values shown are relative bottom-of-the-well energies (ΔE_{rel} in kcal/mol) at the HF/6-31G* level of theory in heptane and water.

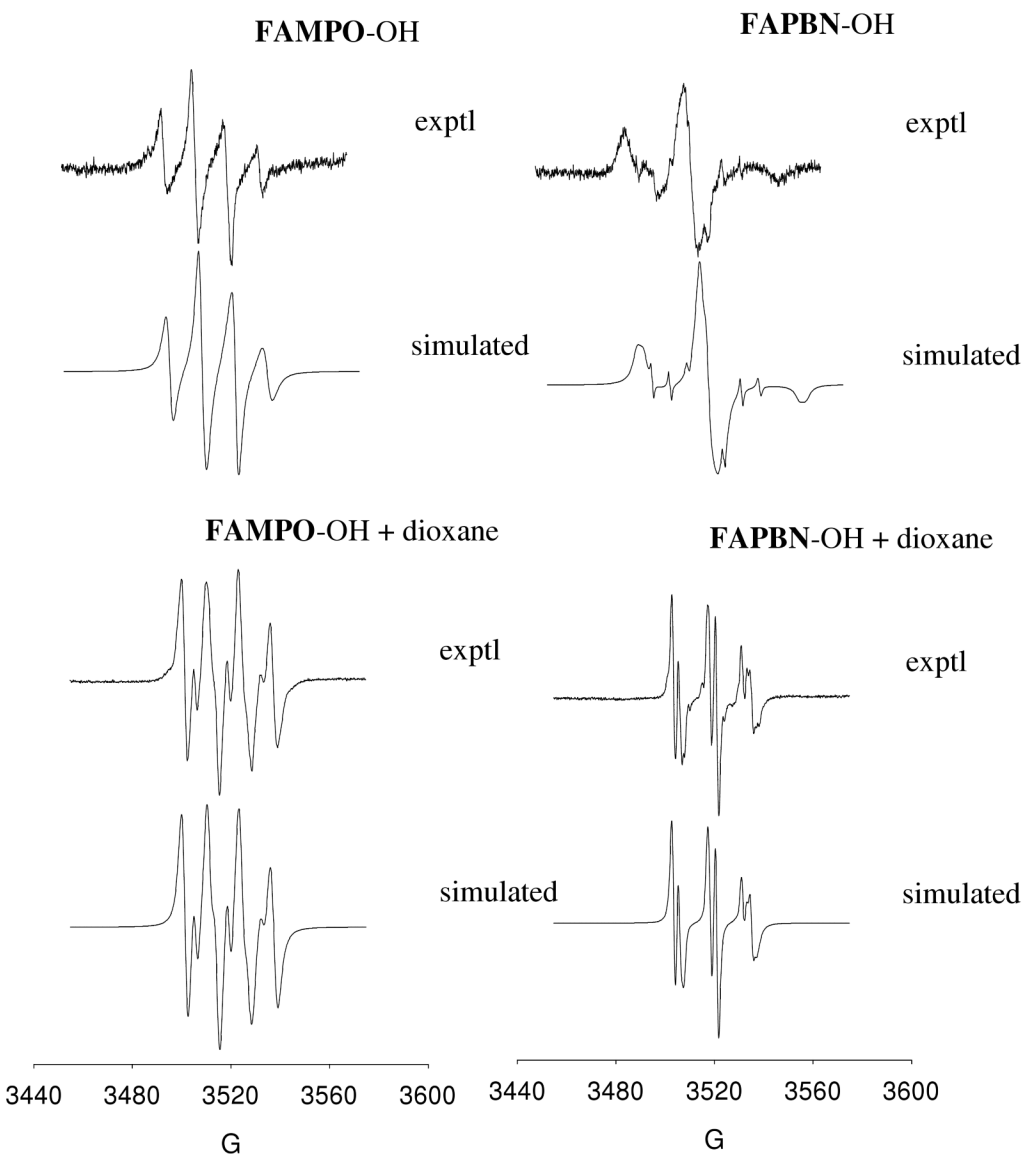

Figure 3.
Experimental and simulated X-band EPR spectra of various hydroxyl adducts of FAMPO and FAPBN in the absence and presence of dioxane in aqueous system.

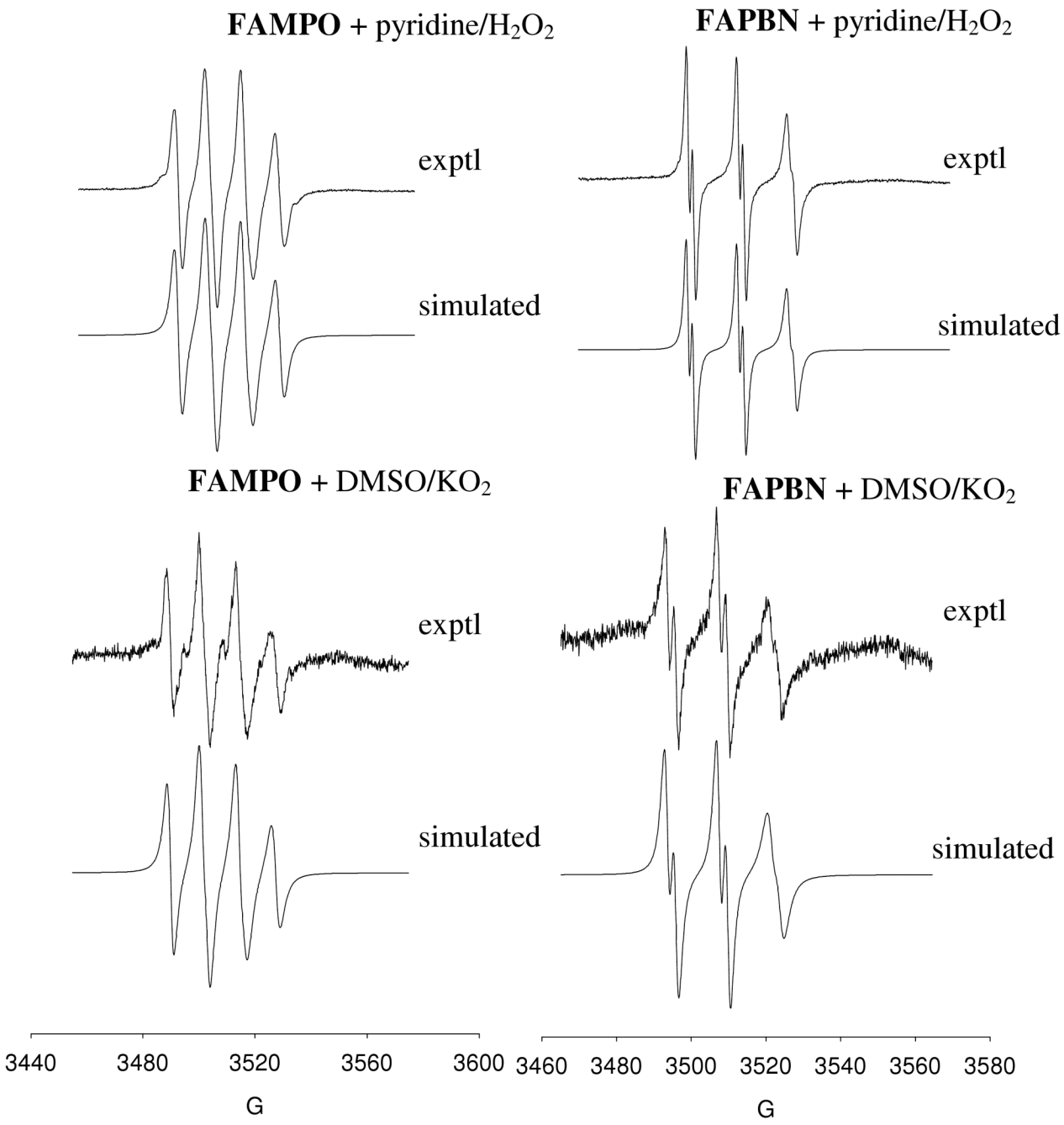

Figure 4.
Experimental and simulated X-band EPR spectra of superoxide radical anion adducts generated from FAMPO and FAPBN using pyridine/H_2O_2 and DMSO/KO_2.

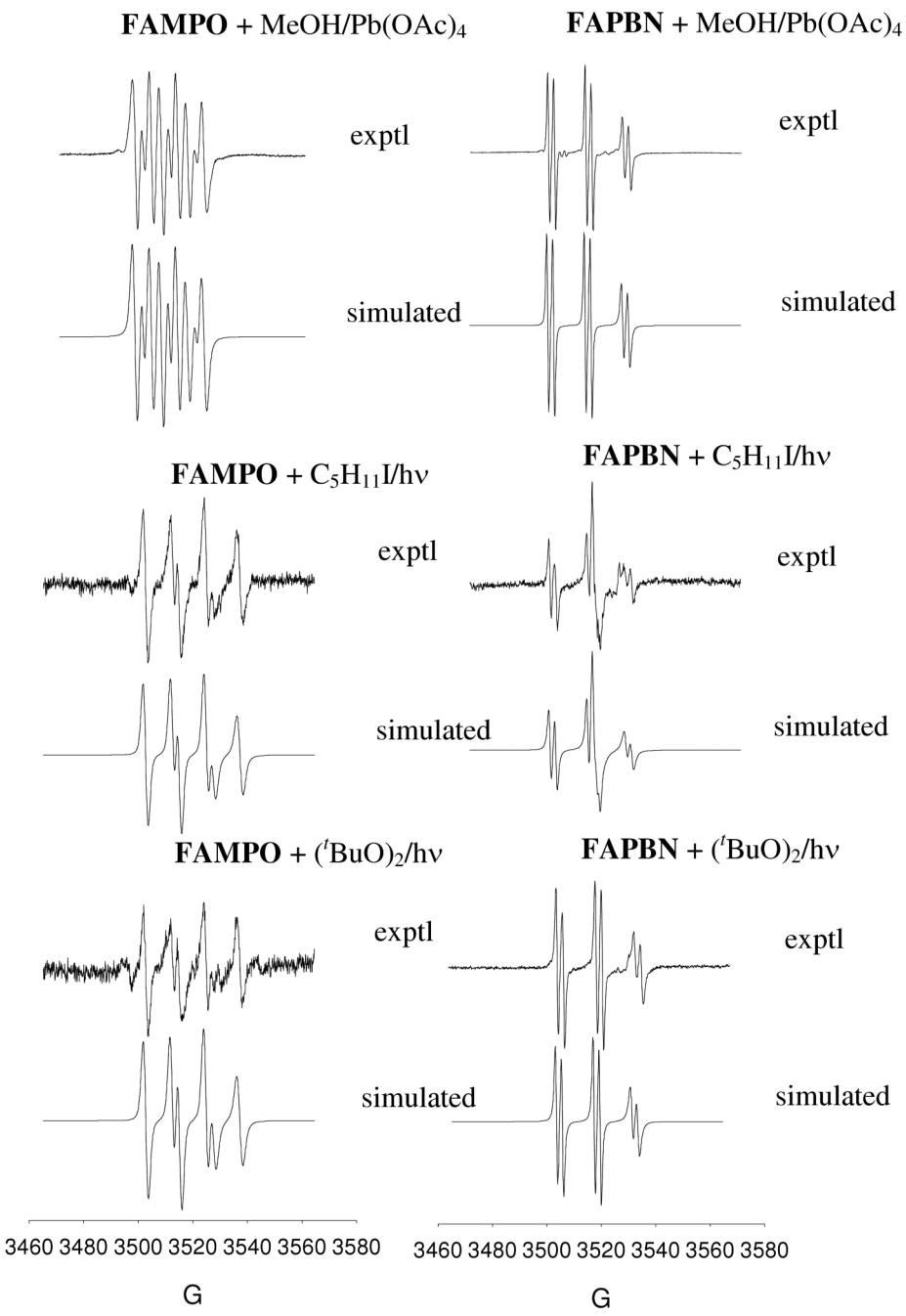

Figure 5.
Experimental and simulated X-band EPR spectra of methoxy, pentyl and *tert*-butoxy radical adducts of FAMPO and FAPBN.

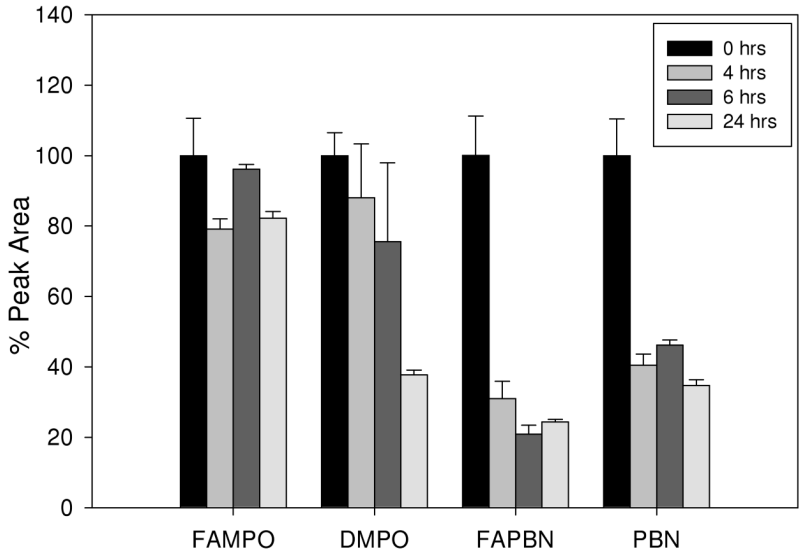

Figure 6.

Concentrations of nitrone compounds after incubation with cells. Cells were incubated with 50 μM of nitrone for 0, 4, 6, and 24 h and the supernatant media was then injected into a HPLC system (see experimental for details). The y-axis corresponds to the % peak area relative to a 50 μM nitrone standard in media. Values represent ± SEM from 2-3 independent experiments.

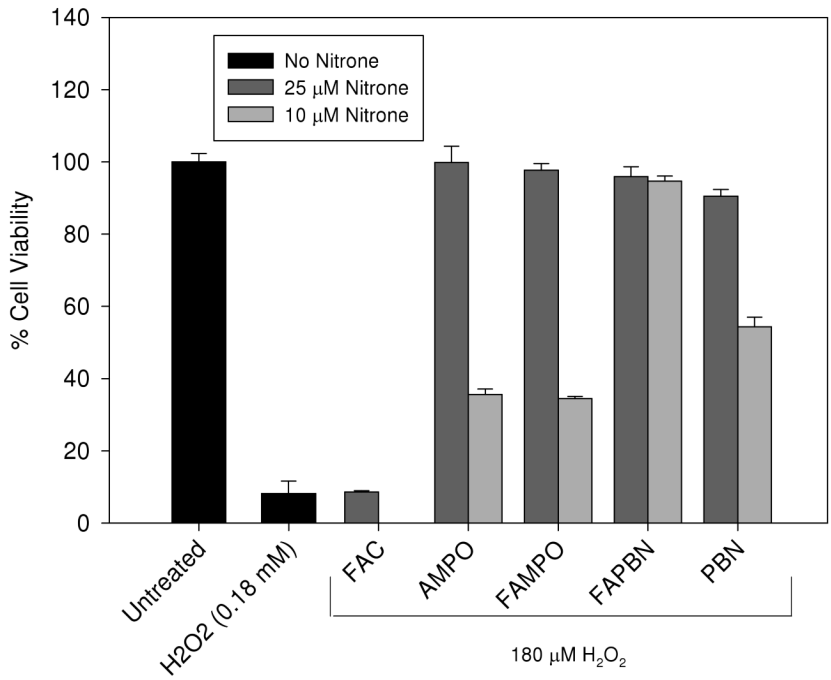

Figure 7.

Cytoprotective property of various nitrones against H_2O_2 toxicity. Cells were incubated in the absence or presence of nitrones for 24 h before being exposed to 180 μM H_2O_2 for another 24 h. Cell viability was measured using MTT assay (see experimental for details). The y-axis corresponds to the % viability relative to untreated cells. *Significantly different from H_2O_2 treatment alone by t-test, $p<0.05$; n = 2-5.

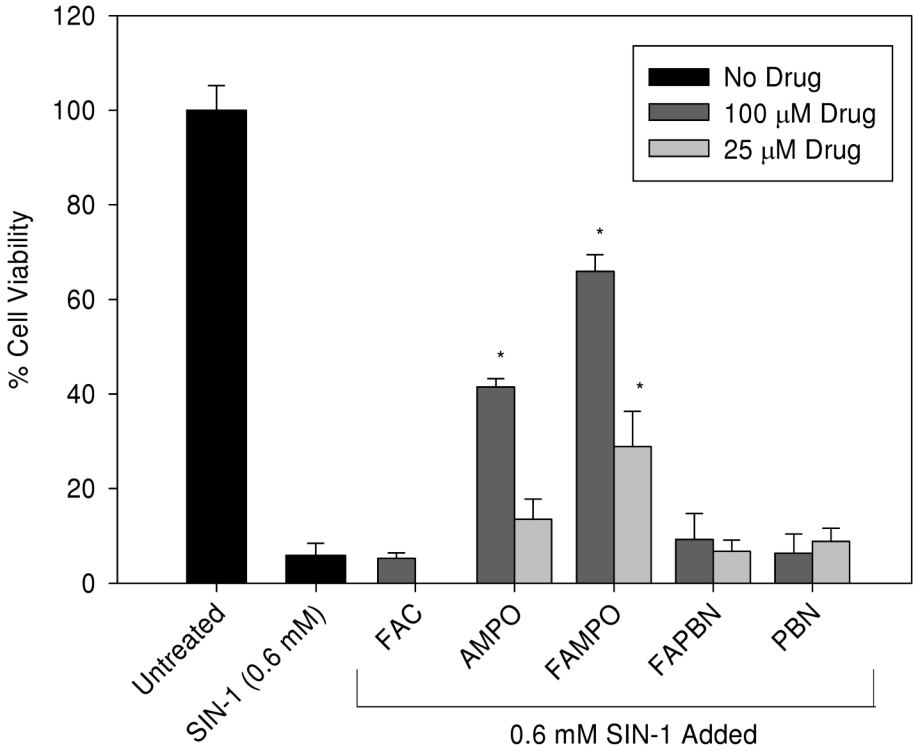

Figure 8.

Cytoprotective properties of various nitrones against SIN-1-induced cell death. Cells were incubated in the absence or presence of nitrones for 24 h before being exposed to 600 μM SIN-1 for another 6 h. Cell viability was measured using MTT assay (see experimental for details). The y-axis corresponds to the % viability relative to untreated cells. *Significantly different from SIN-1 treatment alone by t-test, $p<0.05$. n = 4-10.

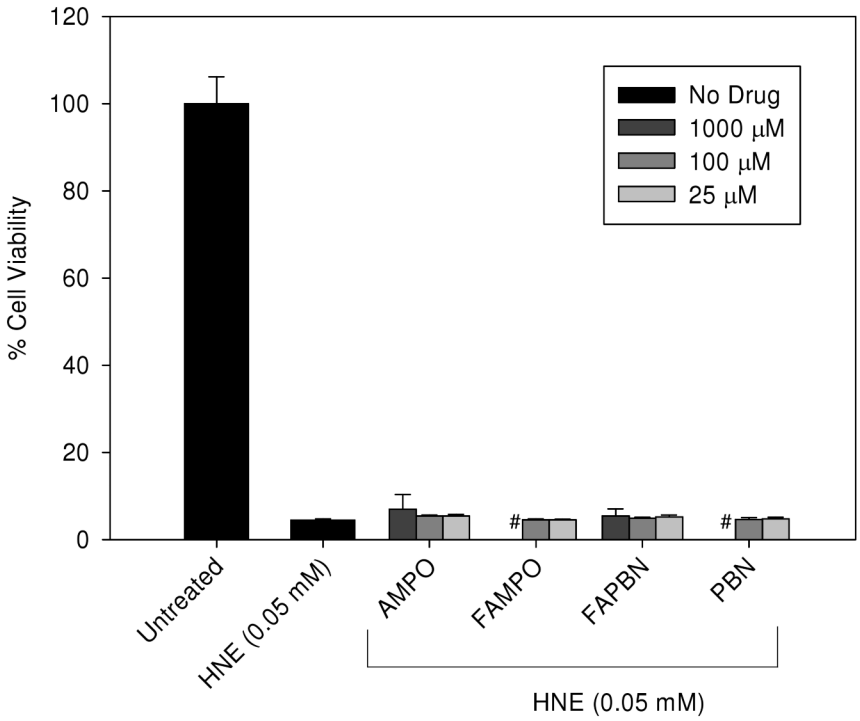

Figure 9.

Cytoprotective properties of various nitrones against HNE-induced cell death. Cells were incubated for 24 h in the presence of nitrones before being exposed to 0.05 mM HNE for another 24 h. Cell viability was measured using MTT assay (see experimental for details). The y-axis corresponds to the % viability relative to untreated cells. See experimental for details. n = 4-5. [#]1 mM FAMPO and PBN were not tested.

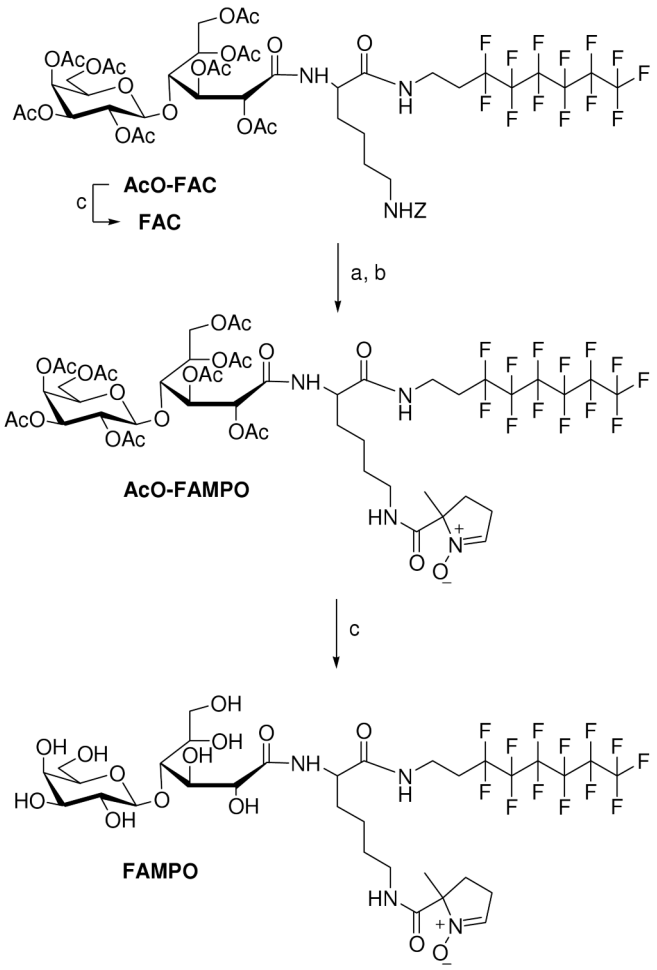

Scheme 1.

Synthesis of FAMPO[a]

[a]Reagents: (a) H_2, 7 bar, Pd/C, ethanol/AcOH 99:1 (*v/v*), 100%; (b) CMPO, EDC, HOBt, TEA, CH_2Cl_2, 67%; (c) NaOMe in anhydrous MeOH, 72%.

Table 1

Lipophilicity of DMPO, PBN, FAMPO and FAPBN.

	DMPO	PBN	FAMPO	FAPBN
log k'_W (RP-HPLC)	0.31[a]	1.64,[a,b] 1.69,[c] 1.75,[d] 1.50,[e]	4.03[a]	5.10,[a] 5.18[c]
log *P* (*n*-octanol/water)	-1.0,[g]	1.2[g]	-	-

[a] This work.

[b] Data from ref (32).

[c] Data from ref (23).

[d] Data from ref (31).

[e] Data from ref (80).

[g] Data from ref (81).

Table 2

Aggregate Sizes of FAPBN and FAMPO in Aqueous Solution

cmpd		concentrations (mM)				
		0.5	**1**	**2.5**	**5**	**10**
FAPBN	D_H [a] (nm)	5.28	5.33	5.53	5.65	5.85
	HHW [b] (nm)	1.35	1.34	1.33	1.32	1.34
	% Vol. [c]	99.5	99.7	99.8	99.8	99.8
FAMPO	D_H [a] (nm)	-[d]	-[d]	5.15	4.59	4.86
	HHW [b] (nm)	-[d]	-[d]	1.45	1.44	1.48
	% Vol.[c]	-[d]	-[d]	100	100	100

[a] D_H: hydrodynamic diameter of particles of the main peak. The values reported are average of 10 measurements.

[b] HHW, the width of the peak at half-height, which is an indication of the degree of polydispersity of the aggregates

[c] Volume particle size distribution.

[d] No stable aggregates were observed.

Table 3

Hyperfine Splitting Constants for FAMPO and FAPBN Radical Adducts.

adduct	source	solvent	FAMPO			FAPBN		
			g	a_N (G)	$a_{\beta\text{-H}}$ (G)	g	a_N (G)	$a_{\beta\text{-H}}$ (G)
HO$^\bullet$	H_2O_2/hν	H_2O	2.0057	13.1	14.3	g_x=g_y= 2.0061[a] g_z = 2.0019	a_x=a_y= 1.2 a_z= 33.0	
HO$^\bullet$	H_2O_2/hν	H_2O + dioxane	2.0058	13.1	9.8	2.0059	13.9	3.5
			2.0058	11.6	13.2	2.0057	15.1	2.5
$O_2^{\bullet -}$	H_2O_2	pyridine	2.0058	12.8	10.6	2.0059	13.5	1.5
$O_2^{\bullet -}$	KO_2	DMSO	2.0058	13.2	13.9	2.0059	13.9	2.3
CH3O$^\bullet$	$CH_3OH/Pb(OAc)_4$	DMSO	2.0058	12.7	0.0	2.0059	13.8	2.2
			2.0058	12.9	7.9			
$^\bullet$C5H11	$C_5H_{11}I$/hν	DMSO	2.0055	12.3	10.0	2.0059	14.0	2.1
						2.0046	-	1.3
^{t}BuO$^\bullet$	$(^t BuO)_2$/hν	DMSO	2.0055	12.3	9.8	2.0059	13.8	2.2

[a] A minor isotropic signal (0.5% cc) can also be seen with g = 2.0056, a_N = 7.3 G, a_H = 29 G.

Table 4

Cytotoxicity of Nitrone Derivatives on Bovine Aortic Endothelial Cells after 24 h of Incubation

cmpd	*% of cell viability*				
	25 μM	**50 μM**	**100 μM**	**500 μM**	**1000 μM**
AMPO	108.3 ± 5.4	109.3 ± 4.6	109.7 ± 5.2	97.1 ± 3.2	95.6 ± 3.2
DMPO	99.9 ± 3.1	100.4 ± 3.0	101.2 ± 1.3	102.2 ± 2.6	99.5 ± 1.1
PBN	99.7 ± 1.4	100.6 ± 1.6	99.0 ± 1.9	100.4 ± 0.9	99.6 ± 3.2
FAMPO	100.3 ± 4.5	106.7±6.6	103.4 ± 3.6	80.0 ± 2.2	47.3 ± 3.0
FAPBN	113.9 ± 7.1	123.0 ± 7.2	104.5 ± 10.2	94.7 ± 4.6	98.0 ± 8.6
FAC	81.7 ± 12.3	78.5 ± 14.6	71.6 ± 14.3	82.6 ± 4.6	5.3 ± 0.4

Cells were incubated for 24 h in the presence of nitrones. Cell viability was measured against untreated cells using MTT assay (see experimental for details. n = 2-4)